sciendo

Technological Forecasting of Deformations in Flat Parts

doi:10.2478/mape-2020-0001

Date of submission to the Editor: 03/2020
Date of acceptance by the Editor: 06/2020

MAPE 2020, volume 3, issue 1, pp. 1-12

Tatiana N. Ivanova
ORCID ID: 0000-0003-2284-2949
Tchaikovsky Branch "Perm National Research Polytechnic Institute", **Russia**
Federal State Budgetary Institution of Science "Udmurt Federal Research Center of the Ural Branch of the Russian Academy of Sciences", Institute of Mechanics, **Russia**

Witold Biały
ORCID ID: 0000-0003-2313-0230
Silesian University of Technology, **Poland**

Jiři Fries
ORCID ID: 0000-0001-9776-6878
VSB-Technical University of Ostrava, **Czech Republic**

Victor Nordin
ORCID ID: 0000-0003-0923-4818
Kaliningrad State Technical University, **Russia**

INTRODUCTION

The strain state in every point of a part is characterized by the relative linear deformations ε_x, ε_y, ε_z, while the stress state is determined by σ_x, σ_y, σ_z (Ivanova, 2016; 2018; 2019; Ivanova et al. 2019; Zakharov et al. 2016; Tyutha et al. 2016; Zitnansky et al. 2013; Davim 2011; 2013; Grote 2011; Fritz & Schulze 2010; Klocke & Konig 2013, Klocke & Kuchle 2011; Groover 2010; Boge 2011; Huo & Cheng 2013; Jackson & Hitchiner 2012; Rowe 2010; Toenshoff & Denkena 2013). Let us analyze two cases of part installation and fastening. In the first scheme of fastening, the plate with width h is machined along its free surface, the plate cannot expand in the directions of the x and z coordinates during processing, i.e. the plate is fixed at the edges, for example, at convergent prisms of a vice. In the second scheme of fastening, the plate is installed on the magnetic base; holding forces in direction of planes are absent, i.e. deformation is not limited by anything.

ORGANIZATION OF THE TEXT

For the first fastening scheme $\varepsilon_x = \varepsilon_z = 0$, so during heating the part will expand only in direction of *y* – axis. The deformation will be:

$$\varepsilon_y = \frac{3\alpha_p q}{\sqrt{\pi a \tau} c \rho} exp\left[-\frac{y^2}{4a\tau}\right] \quad (1)$$

where:

Contact address: tatanic2013@yandex.ru

a – thermal diffusion coefficient;
c – specific heat capacity;
τ – time of contact;
α_p – linear expansion coefficient;
ρ – density of machined material.
The intensity of deformations during uploading is determined the following way:

$$\varepsilon_i = \frac{\sqrt{2}}{3}\sqrt{\left(\varepsilon_y - \varepsilon_x\right)^2 + \left(\varepsilon_x - \varepsilon_z\right)^2 + \left(\varepsilon_z - \varepsilon_y\right)^2} \quad (2)$$

As for the first scheme, $\varepsilon_x = \varepsilon_z = 0$, the intensity of deformation is

$$\varepsilon_{i\,load} = \frac{\sqrt{2}}{3}\sqrt{2\varepsilon_y^2} = \frac{2}{3}\left|\varepsilon_y\right| = \frac{2\alpha_p q}{\sqrt{\pi a \tau}\, c\rho} exp\left[-\frac{y^2}{4a\tau}\right] = 2\alpha_p\theta \quad (3)$$

The intensity of de formations under constant linear expansion coefficient α_p occurs to be directly proportional to the temperature of the point θ. The start of unloading in the given point coincides with the moment of reaching maximum temperature. For the start of unload in git is typical that $\frac{\partial \varepsilon_i}{\partial \tau} = 0$, the stress intensity in this point is described by equation (3). Hence

$$\frac{\partial \varepsilon_i}{\partial \tau} = \frac{\partial}{\partial \tau}\left(2\alpha_p\theta\right) = 2\ \ \alpha_p \frac{\partial \theta}{\partial \tau} = 0 \quad (4)$$

As $\alpha_p \neq 0$, so $\frac{\partial \theta}{\partial \tau} = 0$.
Considering that maxima of temperature θ and deformation intensity ε_i are reached simultaneously, the start of unloading is determined given that:
$\frac{\partial \varepsilon_i}{\partial \tau} = 0$ or $\frac{\partial \varepsilon_i^p}{\partial \tau} = 0$
It is well-known that $\varepsilon_i = \varepsilon_i^e + \varepsilon_i^p$
where:
ε_i^p – plastic component of deformation;
ε_i^e – elastic component of the full intensity of deformation.
The elastic component of deformation for points where it occurs during uploading period, when the intensity of residual stresses is $\sigma_i \geq \sigma_{0,2}$, can be found according the equation:

$$\varepsilon^e = \frac{2(1+\mu)}{3E}, \quad \sigma_i = \frac{2}{3}(1+\mu)\frac{\sigma_{0,2}}{E}$$

where:
μ – Poisson's ratio;
E – elastic modulus;
$\sigma_{0,2}$ – yield strength of machined material.
The dashed line on the Fig. 1 shows how deformation which corresponds to yield strength $\sigma_{0,2}$ changes with the temperature. The ratio $\frac{\sigma_{0,2}}{\mathrm{E}}$ drops with temperature increase and reaches its minimum under θ_{max} in every point, i.e. under $\frac{\partial \theta}{\partial \tau} = 0$. ε_{imax} and ε_{imax}^p occur at the same time (Fig. 1). The change in stress over time is shown in Fig. 2.

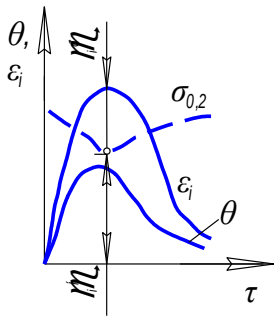

Fig. 1 Dependence of plastic and elastic components of deformation intensity on time

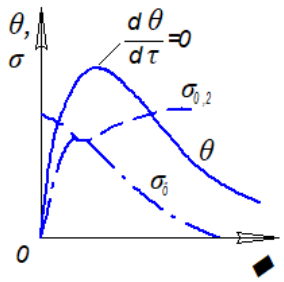

Fig. 2 Dependence of stress at the point of the part on time

To find the moment when the temperature reaches its peak at every point and to determine the time of unloading start, we equate the time derivative of the temperature to zero

$$\frac{\partial\theta}{\partial\tau}=\frac{\partial}{\partial\tau}\left(\frac{q}{\sqrt{\pi\lambda\tau c\rho}}e^{-\frac{y^2}{4a\tau}}\right)=0;\quad \frac{\partial}{\partial\tau}\left(\frac{e^{-\frac{y^2}{4a\tau}}}{\sqrt{\tau}}\right)=0 \tag{4}$$

According to equation (4), the value of heats our ceintensity q does not exert any influence on the position of the moments of unloading start.

To determine the moment of unloading start we find the partial derivative $\frac{\partial\theta}{\partial\tau}$ and set it equal to zero:

$$\frac{\partial}{\partial\tau}\left(\frac{e^{-\frac{y^2}{4a\tau}}}{\sqrt{\tau}}\right)=\frac{e^{-\frac{y^2}{4a\tau}}}{\sqrt{\tau}}+\frac{y^2}{4a\tau^2}-\frac{e^{-\frac{y^2}{4a\tau}}}{2\sqrt{\tau^3}}=0$$

As $\tau\neq 0$ and $e^{-\frac{y^2}{4a\tau}}\neq 0$, it can be assumed that $\frac{y^2}{4a\tau^2}-\frac{1}{2\tau}=0$, or $\frac{y^2}{2a\tau}=1$.

The expression for the start of unloading:

$$\tau_{unload}=\frac{y^2}{2a} \tag{5}$$

Consequently, unloading does not start simultaneously in points of different depth of the part. It was established that for each moment of unloading start and for each point of the depth of the part there is separate pattern of unloading, which is similar to Figure 2.

By inserting the value τ_{unload} into equation (3), we obtain the value of the maximum deformation intensity at the time of unloading. After the transformations we get

$$\varepsilon_{i\,max} = 2\sqrt{\frac{2}{\pi e^{-\frac{y^2}{4a\tau}}}\frac{\alpha_p q}{c\rho}} \cdot \frac{1}{y_l} \tag{6}$$

Equation (6) represents the equation of the equilateral hyperbola. If we draw a curve $\varepsilon_{imax} = f(y)$ and add to this graph a deformation intensity curve $\varepsilon_{i(0,2)}$, which corresponds to the yield strength of the material, the zones of plastic and elastic deformations can be distinguished (Fig. 3).

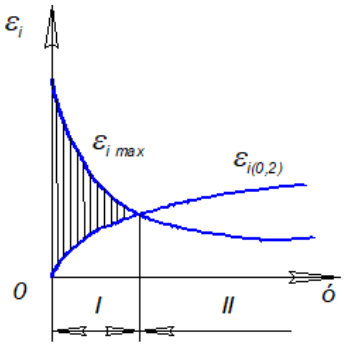

Fig. 3 Scheme for determining the depth of the plastic deformation zone: I – zone of a plastic deformation, II – zone of an elastic deformation

An area, hatched by vertical lines, represents a zone of maximum primary plastic deformations, which penetrate to a depth $y_1\varepsilon_{i(0,2)}$ – an elastic component of deformation intensity, which corresponds to the yield strength $\sigma_{0,2}$.

Considering $\sigma_{i(0,2)} = \frac{\sigma_{0,2}}{3G}$ and $G = \frac{E}{2(1+\mu)}$, we get

$$\varepsilon_{i(0,2)} = \frac{2}{3} \cdot \frac{\sigma_{0,2}}{E}(1+\mu) \tag{7}$$

Plastic deformations occur under the condition: $\varepsilon_i \geq \varepsilon_{i(0,2)}$.

If we assume that $\varepsilon_i = \varepsilon_{i(0,2)}$, we can find the penetration depth of a plastic deformation i.e. y_1

$$y_l = 3\sqrt{\frac{2}{\pi e^{-\frac{y^2}{4a\tau}}}} \cdot \frac{\alpha_p q E}{c\rho\sigma_{0,2}(1+\mu)} \tag{8}$$

Thus, if $y \geq y_1$, the deformation zone is elastic; if $y \leq y_1$, the zone is plastic.

Considering the regularities of heat source intensity dependence on the grinding modes, it can be asserted that with increasing grinding depth and grinding wheel hardness, the value y_1 increases and it decreases with a growth in a speed of the part υ_d and the use of cooling. The higher the heat removal is and the better lubricant properties of the liquid are, the more significant the decrease in y_1 is. Changing these values allows regulation of the residual stresses.

At the end of the process the intensity of residual stresses will be

$$\sigma_{iII} = \left| \frac{2\sigma_{0,2}(1+\mu)}{3E} - 2\sqrt{\frac{2}{\pi e^{-\frac{y^2}{4a\tau}}}} \cdot \frac{\alpha_p q}{yc\rho} \right| \tag{9}$$

During loading up to the moment of unloading compressive stresses occur. At the end of the process in case of cooling until complete detachment residual stresses occurring in the part are tensile ones.

The value of a plastic deformation in the moment of unloading at each point is determined by a difference between complete intensity of deformations ε_{imax} and an elastic component of complete intensity of deformations ε_i^e at the given moment, i.e.

$\varepsilon_{i\ unload}^{p} = \varepsilon_{imax} - \varepsilon_{i(0,2)}$ while $\theta = \theta_{unload}$

By inserting the values ε_{imax} and $\varepsilon_{i(0,2)}$, which were found earlier, into this equation we get

$$\varepsilon_{i\,unload}^{p} = 2\sqrt{\frac{2}{\pi e^{-\frac{y^2}{4a\tau}}}}\cdot\frac{\alpha_p q}{yc\rho} - \frac{2}{3}\cdot\frac{\sigma_{0,2}}{E}(1+\mu) \qquad (10)$$

Calculated deformations during unloading are equal to the difference between complete and plastic deformation in the moment of start of unloading. Marking calculated deformations during unloading by index II, it can be written

$$\varepsilon_{iII} = \left|\varepsilon_i - \varepsilon_{i\,unload}^{p}\right| = \left|2\frac{\alpha_p q}{\sqrt{\pi a\tau}c\rho}e^{-\frac{y^2}{4a\tau}} - 2\sqrt{\frac{2}{\pi e^{-\frac{y^2}{4a\tau}}}}\cdot\frac{\alpha_p q}{yc\rho} + \frac{2}{3}\cdot\frac{\sigma_{0,2}}{E}(1+\mu)\right|$$

Given that $\theta = \theta_{unload}$

The intensity of the calculated deformation is growing with an increase in the heat source intensity.

Given that $\tau \to \infty$, the intensity of residual stresses at the end of the process will be

$$\sigma_{iII} = \left|\frac{2\sigma_{0,2}(1+\mu)}{3E} - 2\sqrt{\frac{2}{\pi e^{-\frac{y^2}{4a\tau}}}}\cdot\frac{\alpha_p q}{yc\rho}\right| \qquad (11)$$

Them a in residual stresses $\sigma_{x\,res}$ or $\sigma_{z\,res}$ are equal to each other; the third main stress, which is perpendicular to the machined (free) surface, is $\sigma_y = 0$. Then

$$\sigma_i = \frac{\sqrt{2}}{2}\sqrt{(\sigma_x-\sigma_y)^2 + (\sigma_y-\sigma_z)^2 + (\sigma_z-\sigma_x)^2} = \frac{1}{2}\sqrt{\sigma_x^2+\sigma_z^2} = |\sigma_x| = |\sigma_z| \qquad (12)$$

Using the ratios from the theory of small el as to plastic deformations:

$\sigma_x - \sigma = \frac{2}{3}\cdot\frac{\sigma_i}{\varepsilon_i}(\varepsilon_x - \varepsilon)$ and $\sigma_y - \sigma = \frac{2}{3}\cdot\frac{\sigma_i}{\varepsilon_i}(\varepsilon_y - \varepsilon)$, and as $\sigma_y = 0$ and $\varepsilon_x = 0$

we subtract the second ratio from the first one and get

$$\sigma_x = \frac{2}{3}\cdot\frac{\sigma_i}{\varepsilon_i}(-\varepsilon_y).$$

But $\varepsilon_i = \frac{2}{3}(\varepsilon_y)$, it means that $\sigma_x = \frac{2}{3}\cdot\frac{\sigma_i}{2/3(\varepsilon_y)}(-\varepsilon_y) = -\sigma_i$.

Consequently, during loading up to unloading moment the stresses have a negative sign, i.e. there are compressive stresses. Speculating about this in that manner, it can be shown that at the end of the process with complete cooling the signs of σ_x and σ_z can be only positive, i.e. residual stresses in the plate before detachment are tensile ones.

In case of the second scheme of fastening $\varepsilon_x = \varepsilon_z \neq 0$. Taking in compressibility condition into account, i.e. when$\varepsilon_x + \varepsilon_y + \varepsilon_z = 3\alpha_p\theta$, we get

$$2\varepsilon_x + \varepsilon_y = \frac{3\alpha_p q}{\sqrt{\pi a\tau}c\rho}\exp\left[-\frac{y^2}{4a\tau}\right] \quad (13)$$

As the plate cannot bend, we take the conditions of symmetry into account and consider that the deformation of all layers is the same, being $\varepsilon_x = \text{const}$.

Thus, considering that $\varepsilon_x = \varepsilon_z \neq 0$, the expression for stress intensity will be:

$$\varepsilon_i = \frac{\sqrt{2}}{3}\sqrt{(\varepsilon_y - \varepsilon_x)^2 + (\varepsilon_x - \varepsilon_z)^2 + (\varepsilon^z - \varepsilon_y)^2} = \frac{\sqrt{2}}{3}\sqrt{2(\varepsilon_y - \varepsilon_x)^2} = \frac{2}{3}|\varepsilon_y - \varepsilon_x| \quad (14)$$

Substituting the difference $\varepsilon_y - \varepsilon_x = 2\varepsilon_x + \varepsilon_y - 3\varepsilon_x$, equation (14) can be demonstrated as

$$\varepsilon_i = \frac{2}{3}|\varepsilon_y - \varepsilon_x| = 2\frac{\alpha_p q}{c\rho\sqrt{\pi a\tau}}\exp\left[\frac{-y^2}{4a\tau}\right] - 2\varepsilon_x \quad (15)$$

The sign of stresses during loading will be as in the first fastening scheme. To be more exact

$$\sigma_x - \sigma = \frac{2}{3}\cdot\frac{\sigma_i}{\varepsilon_i}(\varepsilon_x - \varepsilon);\ \sigma_y - \sigma = \frac{2}{3}\cdot\frac{\sigma_i}{e_i}(\varepsilon_y - \varepsilon).$$

By subtracting the second equation from the first one and considering that for the second scheme $\sigma_y = 0$, we get

$$\sigma_x = \sigma_i\,\mathrm{sh}(\varepsilon_x - \varepsilon_y) = \sigma_y.$$

The moment of unloading start can be found from the condition $\frac{\partial\varepsilon_i}{\partial\tau} = 0$, then

$$\frac{\alpha_p q}{c\rho\sqrt{\pi a}}\left[\frac{e^{-\frac{y^2}{4a\tau}}}{\sqrt{\tau}} + \frac{y^2}{4a\tau} - \frac{e^{-\frac{y^2}{4a\tau}}}{2\tau\sqrt{\tau}}\right] + \frac{\partial\varepsilon_x}{\partial\tau} = 0 \quad (16)$$

If the condition is true in the zone of elastic deformations

$$\varepsilon_x = \alpha_p\theta + \varepsilon_x^e \quad (17)$$

By using the generalized Hooke's law $\varepsilon_x^e = \frac{1}{E}[\sigma_x - \mu(\sigma_y + \sigma_z)]$ and the symmetry of $\sigma_x = \sigma_z$, we get

$$\varepsilon_x^e = \frac{(1-\mu)\sigma_x}{E} \quad (18)$$

By inserting equation (18) in equation (17), we get

$$\varepsilon_x = \alpha_p\theta + \frac{(1-\mu)}{E}\sigma_x.$$

By in targeting this equation with respect to cross-section, the moment of unloading start can be found

$$\tau_{unload} = \frac{e^{-\frac{y^2}{4a\tau}}}{2a\left(e^{-\frac{y^2}{4a\tau}}_{unload} + e^{-\frac{h^2}{4a\tau}}_{unload}\right)} \quad (19)$$

If $h \to \infty$, equation (19) for determining of moment of unloading coincides with the case of the first fastening scheme. Consequently, for thick plates the moments of unloading start are the same in both fastening schemes. As for thin plates, unloading in case of the second scheme starts earlier than in case of the first one. In addition, the thinner the plate is, the earlier unloading begins (Fig. 4).

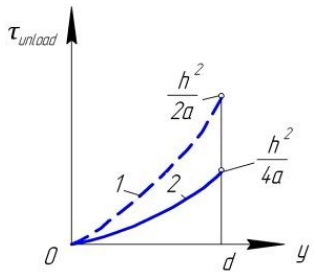

Fig. 4 The time of unloading:
1 – for the first fastening scheme; 2 – for the second fastening scheme

After transformations the value of the deformation intensity at the moment of unloading start for the second fastening scheme will be

$$\varepsilon_i = \left|\frac{2\alpha_p q}{c\rho\sqrt{\pi a\tau}}\exp\left[-\frac{y^2}{4a\tau}\right] - \frac{2\alpha_p q}{hc\rho}\operatorname{erf}\left(\frac{h}{2\sqrt{a\tau}}\right)\right| \quad (20)$$

Inserting the value of τ_{unload} for different layers of a part in formula (19), the graph of deformation intensity can be obtained (Fig. 4).

The value of maximum plastic deformations in the moment of unloading can be found according to the formula

$$\varepsilon^p_{i\,max} = e_{i\,unload} - \frac{2\sigma_{0,2}}{3E}(1+\mu) \quad (21)$$

The boundary of plastic deformation zone can be obtained from the condition

$$\varepsilon_{i\,unload} = \frac{2}{3}\cdot\frac{\sigma_{0,2}}{E}(1+\mu) \quad (22)$$

By comparing equations (22) and (3) it can be demonstrated that at any moment of time the intensity of complete deformations in case of the second fastening scheme will be less than in case of the first one. Moreover, the thinner the plate is, the more significant the difference in values is. It allows us to make a conclusion that in thin plates, fastened according to the second scheme, the deformation intensity at the moment of unloading ε_i is lower than in case of the first scheme of fastening. The temperature in the moments of start of unloading is higher in case of the second scheme, consequently, the value $\varepsilon_{i(0,2)} = \frac{2}{3}\cdot\frac{\sigma_{0,2}}{E}(1+\mu)$ is greater. This is explained by the fact that in the second fastening scheme plastic deformations in the moment of unloading start are lower than in case if the first scheme. In addition, the thinner the part is, the more significant this difference is. As primary plastic deformations govern the values of residual stresses, residual stresses are lower in case of the second scheme. This difference is especially significant in thin plates.

For the process of unloading the calculated deformation intensity is equal to the difference between complete deformation and maximum plastic component of deformation intensity at the moment of start of unloading (Fig. 5).

$$\varepsilon_{iII} = \left|\varepsilon_i - \varepsilon^p_{imax}\right| \text{ or } \varepsilon_{iII} = \varepsilon_{i\,unload} - \frac{2}{3}\cdot\frac{\sigma_{0,2}}{E}(1+\mu) + 2\varepsilon_x \quad (23)$$

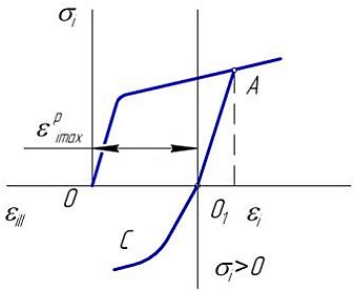

Fig. 5 Change in the position of the coordinate origin due to a change in the direction of loading: O – previous coordinate origin, A – the moment of start of unloading, AO_1 – elastic unloading, O_1 – new coordinate origin, C – new loading

The deformation is always $\varepsilon_x < 0$, it means that in the elastic zone there are only compressive stresses. In the zone, where elastic deformations occurred during loading, we can distinguish two areas. The first one begins from the surface and lasts to a point where $\varepsilon_{iII} = 0$. In this area there are only tensile residual stresses. The second area begins after the point where $\varepsilon_{iII} = 0$, only compressive residual stresses occur in the second area (Fig. 6).

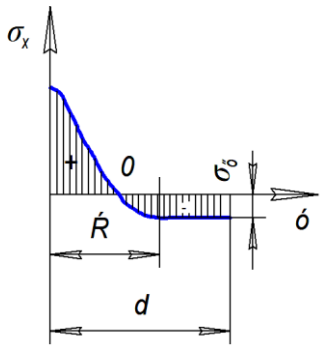

Fig. 6 Stress diagram for the second fastening scheme: A – zone of primary plastic deformations

Compressive stresses are calculated according to the formula

$$\sigma_x = 3\varepsilon_x \frac{E}{(1+\mu)} \tag{24}$$

The process of formation of residual stresses is explained by the scheme, demonstrated on Fig. 7.

The distribution of the temperature in different moments of time τ ang the depth is demonstrated at the top of the Figure.

We assume that considered thin element of the surface layer is separated by a “slit” from the underlying layers of the part. When the grinding wheel passes the considered area of the machined surface at the moment τ_1, its thin layer becomes heated, while the layers below the “slit” stay cold. In this moment the surface layer tends to expand to the value $\alpha_p\theta$, but,being exerted to the resistance of underlying layers, it turns to be plastically compressed. Meanwhile, temporary thermal stresses of compressive nature occur, which causes a plastic deformation of the layer – ε^p. At the moment of time τ_2, when lubricant-cooling

liquid is added, the surface layer cools down and decreases and the stresses become balanced. At the moment of time τ_3, when the part cools down completely, plastically deformed surface layer is exposed to an action of residual tensile stresses due to a resistance to compression from the underlying layers. During machining by the grinding wheel with a discontinuous work surface the part is uniformly heated up to certain depth (Fig. 7a,b).

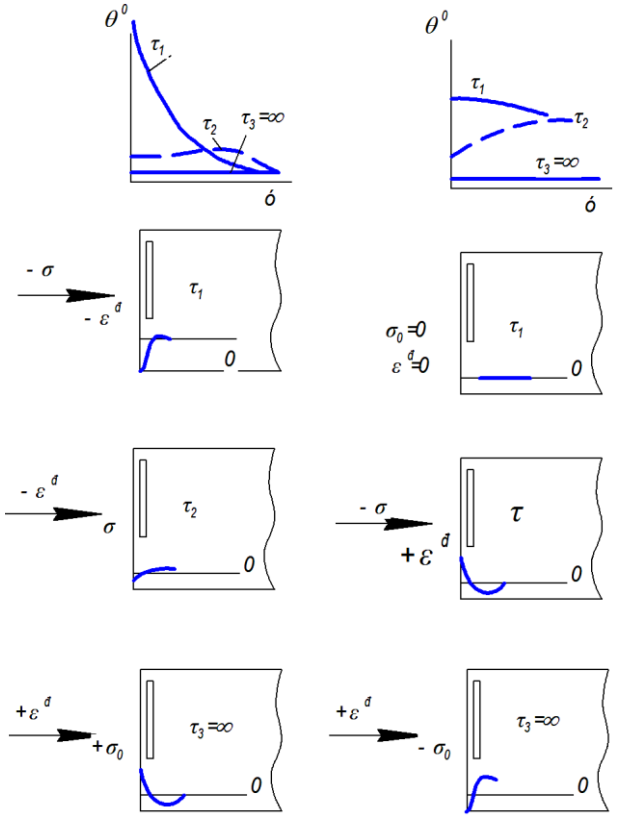

Fig. 7 Scheme of residual stress formation during grinding:
a) the wheel with continuous cutting surface;
b) the wheel with discontinuous cutting surface

Under uniform heating at the momentτ_1 surface layers expand freely and no stresses occur in them. At the next moment of time τ_2 the surface layer, located under the cavity of the wheel, cools down, while the layer below the “slit” stays heated. In this moment the surface layer tending to decrease is exposed to a resistance from the underlying layers. Tensile stresses will cause a plastic deformation $+\varepsilon^p$ in it. Further cooling at the moment of time τ_3 will cause cooling and compression of the subsurface layers, so plastically deformed surface layer will be exposed to an action of compressive residual stresses.

By setting geometric and mechanical characteristics of machined material, one can calculate deformation at each point of a flat part in a software designed with Delphi program language. You can observe the results of the calculation according to equations (1-24) from Fig. 8. It demonstrates a deformation diagram for fastened and loaded flat part with the following characteristics: size

150x10x100 mm; Poisson's ratio 0.30; yield strength 650 MPa; safety factor 2.00.

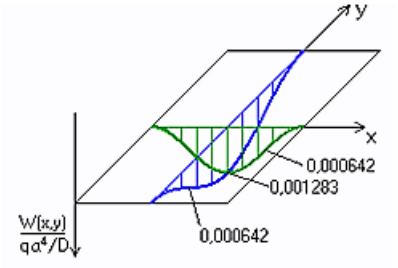

Fig. 8 Deformation of flat part

The value of nonflatness is equal to a sag of span of the plate and it is determined according to the formula

$$C = 0.5\ d^2/\rho \qquad (25)$$

where:

d – diameter of plate,

ρ – radius of plate curvature.

The resulting value of nonflatness is equal to an allowance for nonflatness of plates. If we change the geometric parameters of the part, for example, if we decrease the diameter and reduce under the same other conditions, the curvature of the plate and it almost doubles the allowance for nonflatness of plates. The analysis of the given solution demonstrates that the value of nonflatness from thermal deformations is directly proportional to the initial temperature difference between the plate and bearing surface of the tool, linear expansion coefficient of plate material and its square diameter. At the same time, the value of nonflatness is inversely proportional to the plate thickness. The lower the linear expansion coefficient of material of machined plate is, the higher the probability of oscillations of plate temperature is.

Thus, in order to decrease thermal deformations, it is reasonable to consider the geometric size of a plate to be machined, linear expansion coefficient of plate material and an allowance for nonflatness from thermal deformations.

SUMMARY

As a result of the research on determination of deformations, it is recommended to reduce thermal deformations by considering the geometric size of a plate to be machined, linear expansion coefficient of plate material and an allowance for nonflatness from thermal deformations. The value of nonflatness from thermal deformations is directly proportional to linear expansion coefficient of plate material and its square overall dimensions. At the same time, the value of nonflatness is inversely proportional to the plate thickness.

REFERENCES

Ivanova T.N. (2016). Design and technology support of the grinding process for heavily-machined steel sheets. 2nd International Conference on Industrial Engineering (ICIE-2016). Procedia Engineering. Vol. 150, pp. 782-788. DOI link: https://doi.org/10.1016/j.proeng.2016.07.112

Ivanova T.N. (2018). Structural-technological methods for reduction of thermal stress in grinding. Journal of Engineering Physics and Thermophysics Vol. 91, No. 6, pp. 1485-1490, DOI 10.1007/s10891-018-1874-0

Ivanova T.N. (2019). Thermal stress of abrasive grain during single-pass and multi-pass grinding. Materials Today: Proceedings. https://doi.org/10.1016/j.matpr.2019.07.668.

Ivanova T.N., Bialy W., Nordin V. (2019) Improvement of grinding technology with vortex cooling of steels that are liable to crack propagation. Multidiscilinary Aspects of Production Engineering. Monograph Engineering and Technology. Warszawa. Part 1. p. 9-24

Zakharov O.V., Khudobin L.V., Vetkasov N.I., Sklyarov I.A. and Kochetkov A.V. (2016) Abrasive-Jet Machining of Large Hollow Components. Russian Engineering Research, Vol. 36, Issue 6, pp. 469-471.

Tyuhta A.V., Y Vasilenko. V., Kozlov A.M. (2016) Ways to Enhance Environmental Flat Grinding by Improving the Technology of the Coolant Supply. Procedia Engineering pp. 1073-1080 doi: 10.1016/j.proeng.2016.07.217

Zitnansky J., Zarnovsky J., Ruzbarsky J. (2013). Analysis of physical effects in cutting machining. In: Advanced Materials Research, vol. 801, special iss., p. 51-59.

J. Paulo Davim. (2013). Machining and Machine-Tools Research and Development.

Karl-Heinrich Grote, Jörg Feldhusen. (2011). Dubbel Taschenbuch für den Maschinenbau

Alfred Herbert Fritz, Günter Schulze. (2010). Fertigungstecnik.

Fritz Klocke, Wilfried König. (2013). Fertigungsverfahren 2 Schleifen, Honen, Läppen

F. Klocke, Aaron Kuchle. (2011). Manufacturing Processes 2: Grinding, Honing, Lapping

Mikell P. Groover. (2010). Fundamentals of Modern Manufacturing: Materials, Processes, and Systems.

Alfred Böge. (2011). Handbuch Maschinenbau Grundlagen und Anwendungen der Maschinenbau-Technik

J. Paulo Davim. (2011). Machining of Hard Materials.

Dehong Huo and Kai Cheng. (2013). Micro Cutting Fundamentals and Applications.

Mark J. Jackson, Michael P. Hitchiner. (2012). High Performance Grinding and Advanced Cutting Tools.

W Brian Rowe (2010). Modern Grinding Techniques.

Hans Kurt Toenshoff, Berend Denkena. (2013). Basics of Cutting and Abrasive Processes.

Abstract: The deformation of a part occurring in the process of grinding directly influences its exploitation and quality parameters. The instability of shape and size, which occurs due to an imbalance of residual stress, can be the one of the major causes of deformation of a part. The decrease in stress slows down the deformation process. Considering the regularities of heat source intensity dependence on the grinding modes, it can be asserted that with increasing grinding depth and grinding wheel hardness, the value increases and it decreases with a growth in a speed of the part and the use of cooling. The higher the heat removal is and the better lubricant properties of the liquid are, the more significant the decrease in is. Changing these values allows regulation of the residual stresses. As a result of the research on determination of deformations, it is recommended to reduce thermal deformations by considering the geometric size of a plate to be machined, linear expansion coefficient of plate material and an allowance for nonflatness from thermal deformations. The value of nonflatness from thermal deformations is directly proportional to linear expansion coefficient of plate material and its square overall dimensions. At the same time, the value of nonflatness is inversely proportional to the plate thickness.

Keywords: deformation, stress state is determined, stress diagram, scheme of residual stress formation, grinding